# Solar modulation of AMS-02 daily proton and Helium fluxes with modified force field approximation models

Cheng-Rui Zhu<sup>1, 2</sup> and Mei-Juan Wang<sup>1</sup>

<sup>1</sup>Department of Physics, Anhui Normal University, Wuhu 241000, Anhui, China

<sup>2</sup> Key Laboratory of Dark Matter and Space Astronomy, Purple Mountain Observatory, Chinese Academy of Sciences, Nanjing 210008, Jiangsu, China

### ABSTRACT

As galactic cosmic rays propagate through the turbulent plasma environment within the heliosphere, they undergo a process of diffusion, drift and energy loss, leading to a notable reduction in their flux. This is the solar modulation impact. Recently, the cosmic-ray experiment AMS-02 published daily fluxes of proton and Helium for the period from May 20, 2011 to October 29, 2019 in the rigidity interval from about 1 to 100 GV, exhibiting fine time structures that correlate with solar wind properties on daily basis. In this work, we employ three different modified force field approximation models to fit the data. By fitting to the daily proton and Helium fluxes, we get the time series of solar modulation potential. We find good agreement of data and model predictions for both proton and Helium with the same parameters in two modified force field approximation models. The results in this study verify that the modified FFA model is a valid parametrization of the GCR spectrum also at daily time scales.

### 1. INTRODUCTION

The galactic cosmic rays (GCRs) are charged, energetic particles coming from cosmic accelerators such as supernova remnants, and then propagate diffusively in the Galactic random magnetic field (Moskalenko & Strong 1998). When entering the heliosphere, they encounter a turbulent solar wind with an embedded heliospheric magnetic field (HMF), leading to the local interstellar spectrum (LIS) of GCRs changing into the top-of-atmosphere spectrum (TOA). (Jokipii 1971; Potgieter 2013). This is the solar modulation process of GCRs. Since most of our experiments to detect GCRs are conducted within the heliosphere, this process limits our understanding of GCRs. Consequently, the solar modulation effects are crucial to our understanding of the injection and propagation parameters of cosmic rays, dark matter indirect measurement and the diffusion theory in the galaxy and heliosphere (Bieber 2003; Strong et al. 2007; Blasi 2013; Lavalle & Salati 2012; Yuan & Bi 2015; Boschini et al. 2017; Cui et al. 2017; Tomassetti 2017; Yuan 2018; Zhu et al. 2022).

The basic transport equation (TPE) was derived by Parker (1965); Gleeson & Axford (1967) to describe the GCRs' transport processes in the heliosphere. (Gleeson & Axford 1968) also derived an approximate solution to this TPE, the so called force-field approximation (FFA), which had been widely used as it is simple and enough to explain most of the observations. However, with the advancement of observational technology, the force field approximation increasingly reveals its insufficiencies.

With the successful progress of experiments such as PAMELA, AMS-02, DAMPE (Adriani et al. 2011; Aguilar et al. 2017; Ambrosi et al. 2017), study on cosmic rays has entered an era of high precision. Especially, AMS-02 not only provides high-precision energy spectra for various cosmic ray particles but also offers the temporal evolution of multiple cosmic ray spectra, including protons, Helium, deuterium, He<sup>3</sup>, He<sup>4</sup>, electrons, and positrons. These data have greatly enhanced our understanding of solar modulation. As the FFA cannot explain the data features, people have adopted various methods, including numerical models and modified FFA models to solve this problem. Tomassetti et al. (2018); Luo et al. (2019); Corti et al. (2019); Song et al. (2021); Zhu et al. (2022); Wang et al. (2022) reproduced the AMS observations using a one-dimensional or a three-dimensional numerical model to solve the Parker equation. Several methods have been proposed to expand the FFA (Corti et al. 2016; Cholis et al. 2016; Yuan et al. 2017; Gieseler et al. 2017; Zhu et al. 2021; Shen et al. 2021; Li et al. 2022; Cholis et al. 2022; Long & Wu 2024; Zhu 2024) to account for the differences in observed and predicted GCR spectra.

In the past, we can only study the solar modulation on daily basis with neutron monitors (NMs) (Usoskin et al. 1999; Ghelfi et al. 2017). Recently, the AMS-02 published the daily fluxes of proton and Helium (Aguilar et al. 2021a, 2022) from 1 GV to 100 GV providing new opportunities to study the solar modulation on daily basis based on space-based detector. In this work, we will study these daily fluxes using three modified FFA models that all exhibit rigidity-dependent solar modulation potential.

### 2. METHODOLOGY

## 2.1. Modified force-field approximation models

A full solution to the problem related to CRs transport in the heliosphere is a complicated task and requires sophisticated 3D time-dependent self-consistent modelling (Usoskin 2017). However, the problem can be essentially simplified by the force-field approximation (FFA). The FFA, derived from the Parker transport equation (TPE) (Parker 1965) with several approximations, is widely used due to its simplicity. Usually, the FFA requires the quasi-steady changes, spherical symmetry, etc, witch are apparently invalid for short time scales. In fact, they are not fully valid even for the regular condition (Caballero-Lopez & Moraal 2004). However, the force-field formalism was found to provide a very useful and comfortable mathematical parametrization of the GCR spectrum even during a major Forbush decrease (FD), irrespective of the (in) validity of physical assumptions behind the force-field model. So one can still benefit from the simple parametrization offered by the FFA for practical uses other than studying the physics of solar modulation, even if the FFA is not a physically motivated solution to the solar modulation problem at daily time scales. (Usoskin et al. 2015). In the FFA model, the TOA flux is related with the LIS flux as

$$J^{\text{TOA}}(E) = J^{\text{LIS}}(E + \Phi) \times \frac{E(E + 2m_p)}{(E + \Phi)(E + \Phi + 2m_p)},\tag{1}$$

where E is the kinetic energy per nucleon,  $\Phi = \phi \cdot Z/A$  with  $\phi$  being the solar modulation potential,  $m_p = 0.938$  GeV is the proton mass, and J is the differential flux of GCRs. The only parameter in the force-field approximation is the modulation potential  $\phi$ .

With the development of instruments, the observational data shows that we cannot fit the cosmic ray flux well with just one parameter, therefore, an rigidity-dependent solar modulation potential is needed (Gieseler et al. 2017; Siruk et al. 2024). Several methods have been proposed to describe the rigidity-dependent of solar modulation potential, such as Shen et al. (2021); Cholis et al. (2022); Long & Wu (2024); Zhu (2024). In this work we describe the rigidity-dependent of solar modulation potential with three different modified FFA models. First, the solar modulation potential in Zhu's model (Zhu 2024) is shown as

$$\phi(R)_{Zhu} = \phi_l + \left(\frac{\phi_h - \phi_l}{1 + e^{(-R + R_b)}}\right) \tag{2}$$

where  $\phi_l$  is the solar modulation potential for the low energy, and  $\phi_h$  is for the high energy, e is the natural constant, R is the rigidity and  $R_b$  is the break rigidity. This model is developed from the model in Corti et al. (2016).

Second, Cholis' model from Cholis et al. (2016); Cholis & McKinnon (2022) is described as

$$\phi(R)_{Cholis} = \phi_0 + \phi_1 \left( \frac{1 + (R/R_0)^2}{\beta (R/R_0)^3} \right). \tag{3}$$

Here,  $\beta$  is the ratio between the particle speed and the speed of light.  $\phi_0$ ,  $\phi_1$  and  $R_0$  are the free parameters to be fitted. In the original Cholis model,  $\phi_0$  and  $\phi_1$  are parameters that depend on the magnetic field intensity (B) and tilt angle  $(\alpha)$ . We allow these parameters to vary freely in order to obtain better fitting results.

Third, Long's model from Kuhlen & Mertsch (2019); Long & Wu (2024) is described as

$$\phi(R)_{Long} = \phi_0 + \phi_1 \ln(R/R_0),\tag{4}$$

with

$$J^{\text{TOA}}(E) = J^{\text{LIS}}(E + \Phi(R)) \times \frac{E(E + 2m_p)}{(E + \Phi(R))(E + \Phi(R) + 2m_p)} exp(-g \frac{10R^2}{1 + 10R^2} \phi(R))). \tag{5}$$

Here,  $\phi_0$ ,  $\phi_1$  and g are the free parameters to be fitted with  $\Phi(R) = \phi(R) \cdot Z/A$ .

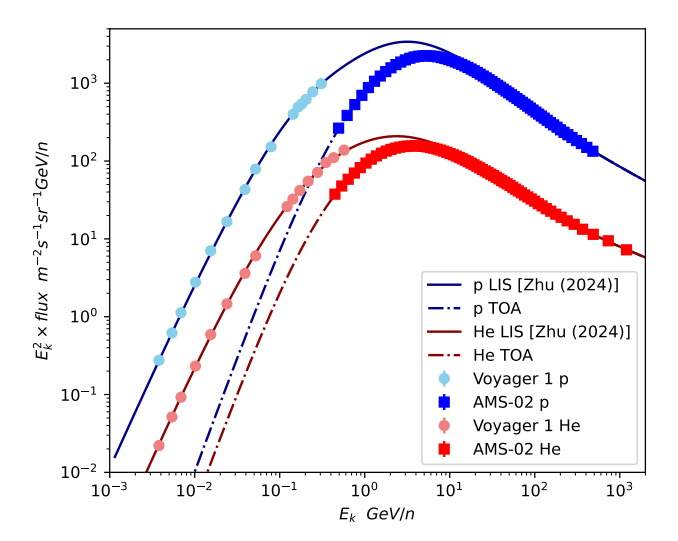


Figure 1. LIS fluxes (lines) and TOA fluxes (dashed lines) of p and He from Zhu (2024), multiplied by  $E_k^2$ , compared with the measurements (colorful points) of Voyager 1 (Cummings et al. 2016), and AMS-02 (Aguilar et al. 2021b).

There are different p and He LIS assumption in the literature, such as Potgieter (2014); Ghelfi et al. (2016); Corti et al. (2016); Boschini et al. (2018); Zhu (2024). In this work, we take the LIS from our previous work Zhu (2024), where we get the LIS with the cubic spline interpolation method, with the highest-order of polynomial of three, and we still assume Z/A=1/1 for proton and Z/A=2/4 for He. The LISs for proton and Helium are shown in Fig. 1.

We use the Markov Chain Monte Carlo (MCMC) algorithm to find the best fitting results, which works in the Bayesian framework. The posterior probability of model parameters  $\theta$  is given by

$$p(\boldsymbol{\theta}|\text{data}) \propto \mathcal{L}(\boldsymbol{\theta})p(\boldsymbol{\theta}),$$
 (6)

where  $p(\theta)$  is the prior probability of  $\theta$ , and  $\mathcal{L}(\theta)$  is the likelihood function of parameters  $\theta$  given the observational data. Here,  $\mathcal{L}(\theta) = exp(-\chi^2/2)$ , with  $\chi^2$  is the defined as

$$\chi^{2} = \sum_{i=1}^{m} \frac{\left[J(E_{i}; \phi_{l}, \phi_{h}, R_{b}) - J_{i}(E_{i})\right]^{2}}{\sigma_{i}^{2}},\tag{7}$$

where  $J(E_i; \phi_l, \phi_h, R_b i)$  is the expected flux,  $J_i(E_i)$  and  $\sigma_i$  are the measured flux and error for the *i*th data bin with geometric mean energy  $E_i$ .

The MCMC driver is adapted from CosmoMC (Lewis & Bridle 2002; Liu et al. 2012). We adopt the Metropolis-Hastings algorithm. The basic procedure of this algorithm is as follows. We start with a random initial point in the parameter space, and jump to a new one following the covariance of these parameters. The accept probability of this new point is defined as min  $[p(\theta_{\text{new}}|\text{data})/p(\theta_{\text{old}}|\text{data}), 1]$ . If the new point is accepted, then repeat this procedure from this new one. Otherwise go back to the old point. For more details about the MCMC one can refer to (Gamerman 1997).

### 3. RESULTS AND DISCUSSION

Based on the MCMC method, we simultaneously fit the daily flux spectra of protons, Helium, and the proton-to-Helium ratio using three modified models compared to the FFA. The  $\chi^2/d.o.f$  for them are shown in Fig. 2. Consistent with previous studies, the FFA model failed to explain the time-dependent cosmic ray spectra. The FFA shows  $\chi^2/d.o.f$ 

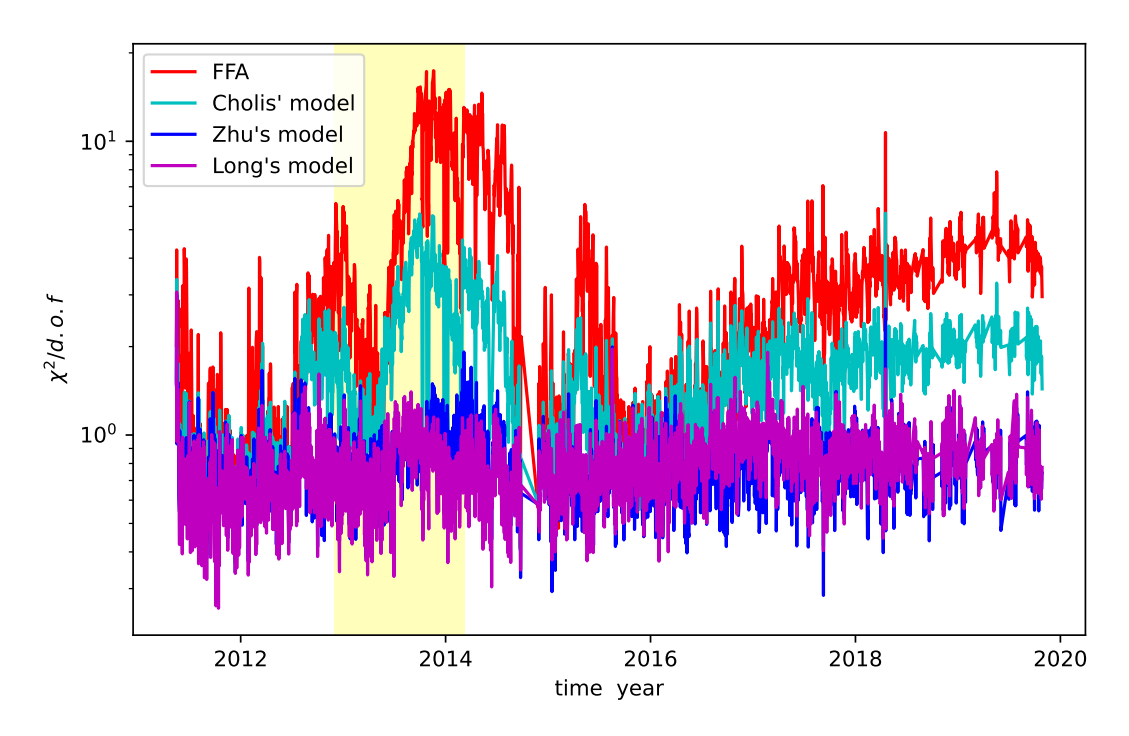


Figure 2. The  $\chi^2/d.o.f$  for the Cholis' model (cyan line), Zhu's model (red line) and Long's model (magenta line) compared to the FFA (red line). The d.o.f for the three modified FFA models are the same, while the d.o.f for the FFA are two greater than theirs. The yellow band stands for the heliospheric magnetic field reversal period within which the polarity is uncertain(Sun et al. 2015).

with values from 0.366 to 17.396 and mean value being 3.293. That's why we need a modified FFA models to describe the solar modulation effect. As shown in (Long & Wu 2024), the Cholis' model fits the time-dependent proton and Helium fluxes better than the FFA, but it still has significant discrepancies during the solar polarity reversal phase and after 2016. The  $\chi^2/d.o.f$  values for the Cholis' model range from 0.367 to 5.690, with an average value of 1.629. The Zhu's model and Long's model exhibit similar fitting results, with the Long's model being slightly better. The mean  $\chi^2/d.o.f$  values for Zhu's model values for Zhu's model are 0.805, ranging from 0.284 to 3.004. There are 18 days with a  $\chi^2/d.o.f$  value greater than 1.5 in the Zhu's model, which accounts for 6.4‰ of the data, and most of them arise around 2014 when the heliospheric magnetic field polarity is uncertain. The mean  $\chi^2/d.o.f$  values for Long's model are 0.793, ranging from 0.257 to 3.068, and there are 11 days with a  $\chi^2/d.o.f$  value greater than 1.5 in the Long's model. Hereafter, we will present the fitting results of Zhu and Long's models. We checked that the days with  $\chi^2/d.o.f > 1.5$  for both Zhu's and Long's models are not correlated with Forbush decrease days listed in Wang et al. (2023) and in the IZMIRAN database <sup>1</sup>.

In the Zhu's model, the  $\phi_l$ ,  $\phi_h$  and  $R_b$  are time-varying parameters to be fitted and MCMC is performed to fit the daily data of proton, Helium and p/He ratio together. In Fig. 3, we show the fitting result, and all the specific values are provided in Table. 1. The amplitude of  $\phi_h$  series is samller than of  $\phi_l$ , and it means the low rigidity particles are more sensitive to the solar activities. The Zhu's model is overfitting in some cases, as indicated by the large uncertainties in the fitted parameters, especially in 2012 and 2016. In these cases, we have that  $\phi_l$  and  $\phi_h$  are consistent with each other and/or that  $R_b$  is consistent with zero, i.e., no break is effectively present. This means that when the Zhu's model overfits, it essentially reverts to the FFA behavior, as indicated also by the fact that the  $\chi^2/d.o.f$  for these days is very similar between the Zhu's model and the FFA fits.

http://spaceweather.izmiran.ru/eng/dbs.html

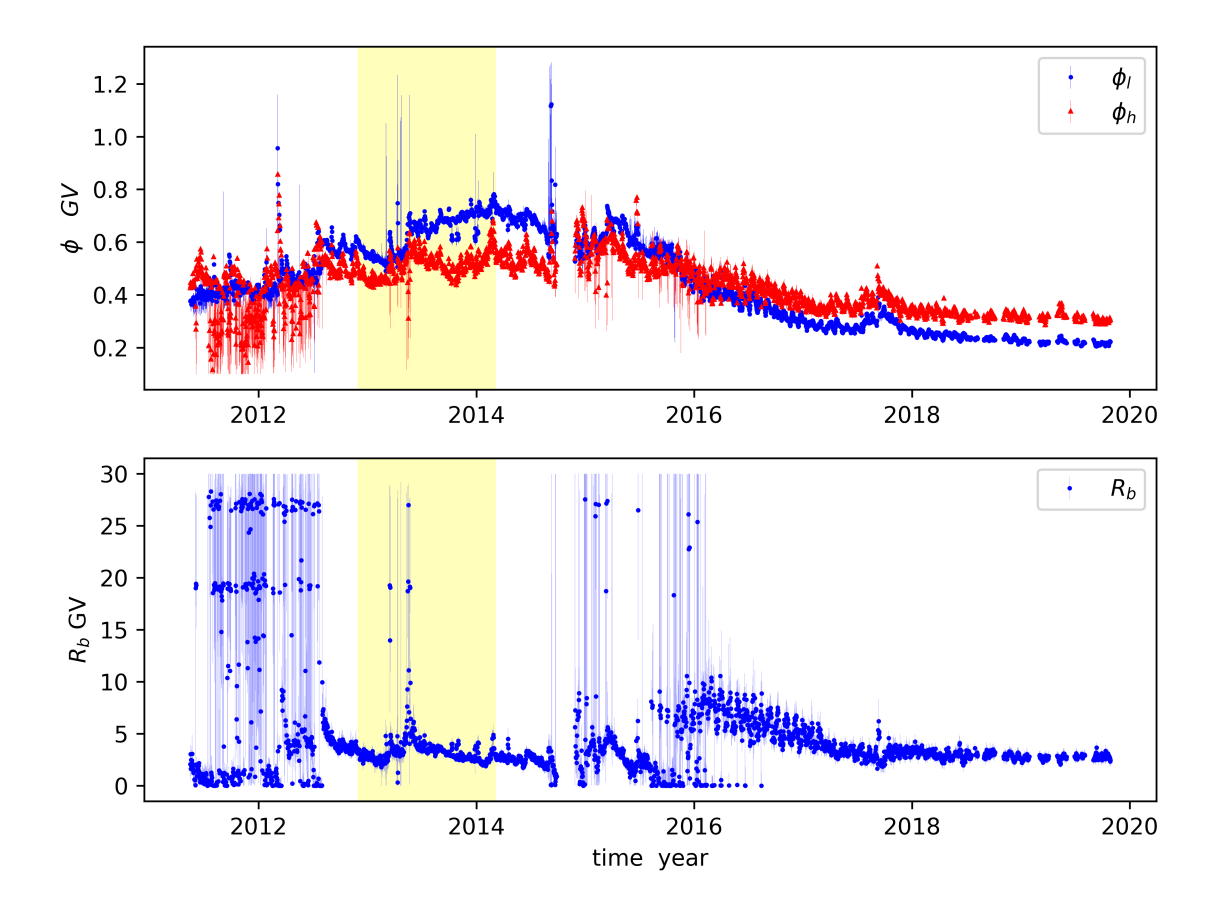


Figure 3. (Top) Time series of  $\phi_l$  (blue marker) and  $\phi_h$  (red marker) via fitting to the AMS-02 p, He and p/He from 2011 to 2019. (Bottom) Same to the top but for  $R_b$ . The yellow band stands for the heliospheric magnetic field reversal period within which the polarity is uncertain(Sun et al. 2015).

**Table 1.** The results derived with AMS-02 daily data using Zhu's model. This table is available in its entirety in machine-readable form.

date	$\phi_l \text{ (GV)}$	$\phi_h \text{ (GV)}$	$R_b$ (GV)	$\chi^2/d.o.f$
	$\begin{array}{c} 3.704 \mathrm{e}\hbox{-}01^{+1.396 e}\hbox{-}02 \\ -3.236 e}\hbox{-}02 \\ 3.757 \mathrm{e}\hbox{-}01^{+8.338 e}\hbox{-}03 \\ -1.325 e}\hbox{-}02 \\ 3.683 \mathrm{e}\hbox{-}01^{+1.865 e}\hbox{-}02 \\ 3.751 \mathrm{e}\hbox{-}01^{+1.061 e}\hbox{-}02 \\ 3.752 \mathrm{e}\hbox{-}01^{+1.24 e}\hbox{-}02 \\ \end{array}$	$\begin{array}{c} 4.254 \mathrm{e}\hbox{-}01^{+1.192 e}\hbox{-}02 \\ -9.830 e \hbox{-}03 \\ 4.489 \mathrm{e}\hbox{-}01^{+1.499 e}\hbox{-}02 \\ -1.304 e \hbox{-}02 \\ 4.356 \mathrm{e}\hbox{-}01^{+9.391 e}\hbox{-}03 \\ 4.279 \mathrm{e}\hbox{-}01^{+1.287 e}\hbox{-}02 \\ -1.011 e \hbox{-}02 \end{array}$	$\begin{array}{c} 2.747\mathrm{e} + 00^{+1.149e + 00}_{-1.329e + 00} \\ 4.032\mathrm{e} + 00^{+9.356e - 01}_{-9.951e - 01} \\ 2.242\mathrm{e} + 00^{+1.056e + 00}_{-1.361e + 00} \\ 3.290\mathrm{e} + 00^{+1.259e + 00}_{-1.127e + 00} \end{array}$	1.482e+00 3.004e+00 9.322e-01 1.835e+00
$2011/5/24 \\ 2011/5/25$	$3.563e-01_{-3.185e-02}^{+1.608e-02} 3.786e-01_{-2.150e-02}^{+1.083e-02}$	$4.284e-01_{-8.916e-03}^{+1.036e-02}  4.314e-01_{-1.143e-02}^{+1.450e-02}$	$2.513e + 00^{+9.054e - 01}_{-9.765e - 01}$ $3.492e + 00^{+1.504e + 00}_{-1.385e + 00}$	1.158e+00 1.430e+00

We show the model predictions compared to the AMS-02 daily data in Fig. 4, 5 and 6 from 2011 to 2019. The figures show that the fitting agrees with the data within  $\pm$  %5. The fitting of proton is better, as most of the fits agree with the data within  $\pm$  %2. After 2017 the model predicts higher fluxes around 10 GV for both p and He. For He, it predicts higher fluxes around 3 GV at all times, and lower fluxes at  $\sim$  2 GV after 2017. For p, there are long periods of higher predicted fluxes at 1 GV. These small discrepancies in the p and He fluxes are reflected in the He/p ratio, with slight systematic overpredictions at 2 GV and underpredictions at 3 GV.

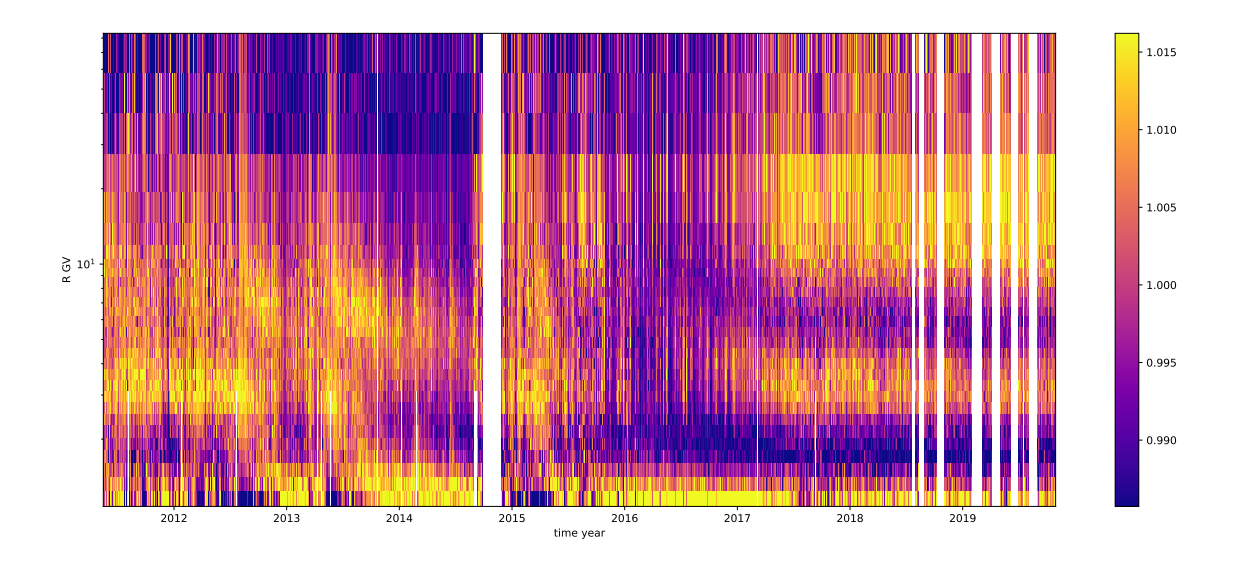


Figure 4. The ratio of Zhu's model prediction to data (model/data) for p fluxes of AMS-02 from 2011 to 2019.

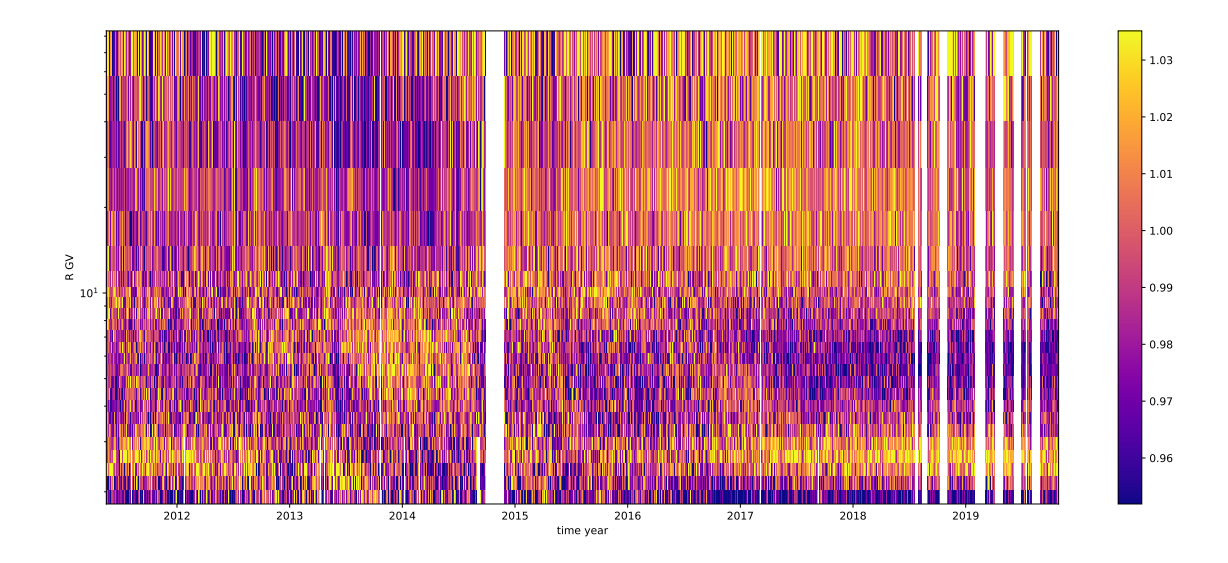


Figure 5. Same as 4 but for He.

The  $\phi_0$ ,  $\phi_1$  and g are the free parameters to be fitted in Long's model and the fitting results of them are shown in Fig. 7, and all the specific values are provided in Table. 2. We set the parameter g range from -0.2 to 0.2 in the MCMC. The results show that the best-fit g values are on the upper edge, especially in the years 2014, 2016, and 2017. If we expand the range of g, the  $\chi^2/d.o.f$  will be slightly smaller with mean value changes from 0.793 to 0.755, and g will become larger. The uncertainty of these three parameters will also increase. These behaviors may be caused by the overfitting of Long's model here.

The Long's model predictions compared to the AMS-02 p, He and p/He ratio data from 2011 to 2019 are shown in Fig. 8, 9 and 10. Similar to the Zhu's model, most of the predictions agree with the data within  $\pm 5\%$ . The behavior of

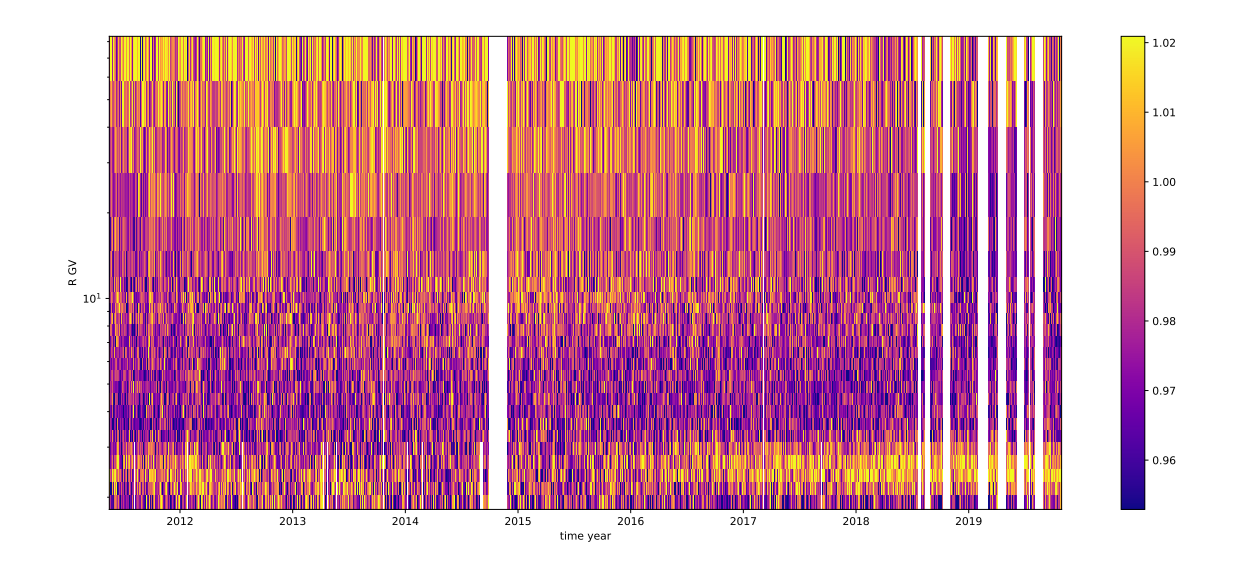


Figure 6. Same as 4 but for ratio of He/p.

Table 2. The results derived with AMS-02 daily data using Long's model. This table is available in its entirety in machine-readable form.

date	$\phi_0 \text{ (GV)}$	$\phi_1 \text{ (GV)}$	g	$\chi^2/d.o.f$
2011/5/20	$3.715e-01^{+8.047e-03}_{-7.927e-03}$	$3.831e-02^{+1.254e-02}_{-1.281e-02}$	$-3.367e-02^{+2.733e-02}_{-2.322e-02}$	1.504e+00
2011/5/21	$3.606e-01^{+7.547e-03}_{-7.352e-03}$	$4.228e-02^{+1.138e-02}_{-1.231e-02}$	$-1.316e-02^{+2.691e-02}_{-2.227e-02}$	3.068e + 00
2011/5/22	$3.795 \text{e-} 01^{+7.410e-03}_{-7.480e-03}$	$3.325e-02^{+1.151e-02}_{-1.246e-02}$	$-1.118e-02^{+2.690e-02}_{-2.213e-02}$	9.498 e-01
2011/5/23	$3.701e-01^{+7.435e-03}_{-7.146e-03}$	$2.802e-02^{+1.139e-02}_{-1.284e-02}$	$-2.750e-03^{+3.048e-02}_{-2.449e-02}$	1.855e + 00
2011/5/24	$3.619e-01^{+7.739e-03}_{-7.793e-03}$	$4.567e-02^{+1.197e-02}_{-1.156e-02}$	$-3.383e-02^{+2.343e-02}_{-2.164e-02}$	1.184e + 00
2011/5/25	$3.722e-01_{-7.445e-03}^{+7.125e-03}$	$2.768e-02^{+1.213e-02}_{-1.217e-02}$	$-2.362 \text{e-} 03^{+2.892e-02}_{-2.459e-02}$	1.439e+00

model/data is also similar to Zhu's. Except for the proton fluxes, Long's fitting results are slightly worse than Zhu's. And there are long periods of smaller predicted fluxes before 2017 and high predicted fluxes after that at 1 GV for p. In Fig. 11, we present the time profile of the Helium-to-proton ratio (He/p) for several rigidity values from Zhu and Long's model. Using the same modulation parameters for both p and He, the ratio of He/p can be fitted very well. The two models both successfully reproduced the time evolution of He/p from 2011 to 2019. We show the He/p ratio at R = 0.5 GV and 1.077 GV where there is no ASM-02 data. At R = 0.5 GV, Long's model predicts a higher He/p ratio than Zhu's model in 2014, and a lower ratio after 2017. At R = 1.077 GV, the situation is the opposite. At higher rigidities, Long's model prediction is very similar to Zhu's model prediction. At the rigidity R = 0.5 GV, the He/p increase from 2011 to 2014 with increasing of solar activity, and then decrease to low values in 2014–2019. At higher rigidities, the behavior is completely opposite. At even higher rigidities, the He/p ratio will not change with time. The long-term behavior of the He/p ratio at the low rigidities is caused by two reasons: the different Z/A value and LIS for p and He as discussed in our previous work (Zhu 2024) as they share the same solar modulation parameters. For more information about this one can refer to Zhu (2024).

### 4. CONCLUSION

The precise measurements of daily cosmic ray proton and Helium spectra by AMS-02 between 2011 to 2019 provide an important chance to improve our understanding for the solar modulation. In this paper, we fit the daily p, He and p/He data from AMS-02 with three modified FFA models and FFA model. We find that, using the non-parametric LIS from Zhu (2024) for proton and Helium, we can fit the data very well with two modified FFA models, Zhu's model

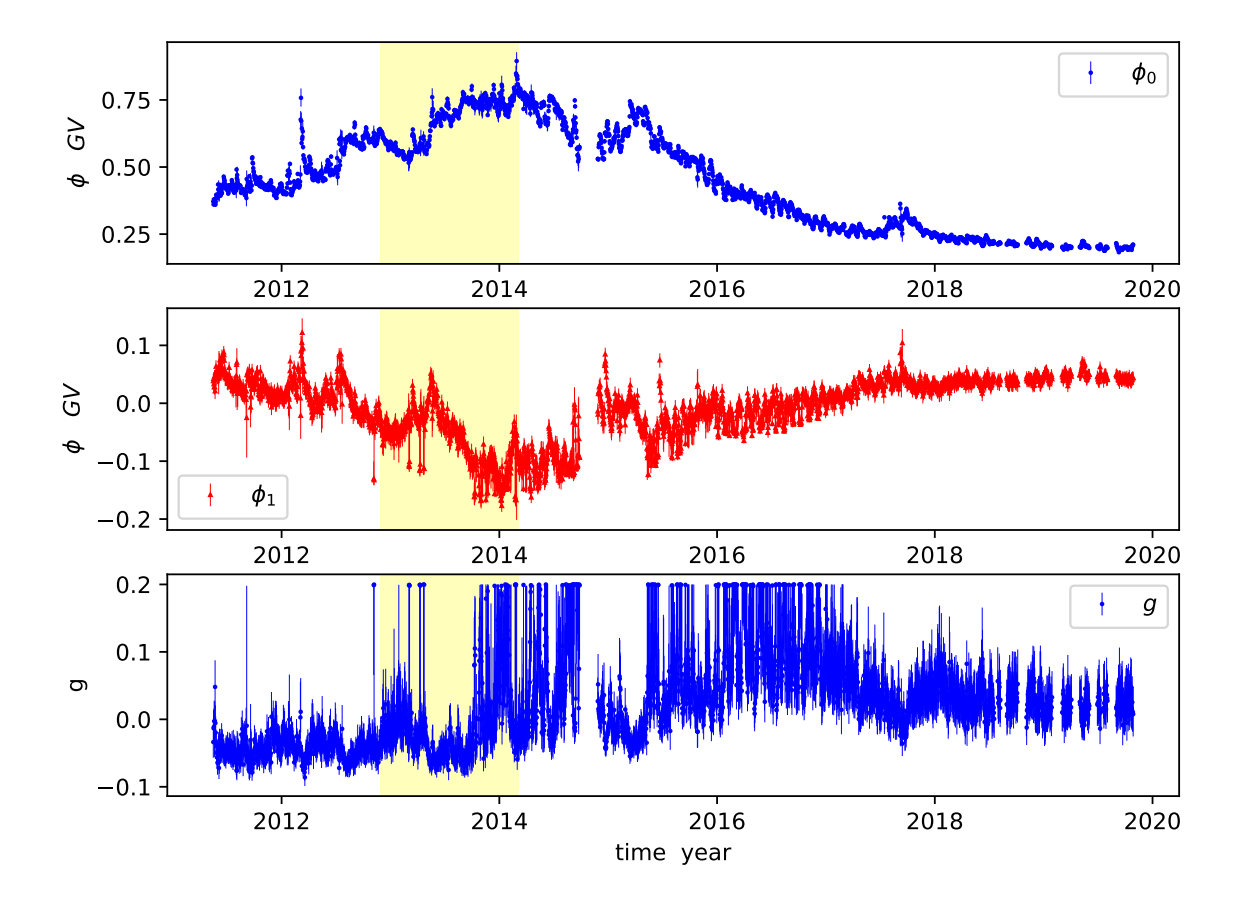


Figure 7. (Top) Time series of  $\phi_0$  in Long's model via fitting to the AMS-02 p, He and p/He from 2011 to 2019. (Middle) Same to the top but for  $\phi_1$ . (Bottom) Same to the top but for g. The yellow band stands for the heliospheric magnetic field reversal period within which the polarity is uncertain(Sun et al. 2015).

and Long's model. In the Zhu's model, a sigmoid function is used to replace the constant  $\phi$  in the FFA. The sigmoid function has three parameters,  $\phi_l$  for low rigidity,  $\phi_h$  for high rigidity and  $R_b$  for the break rigidity. The evolution of  $\phi_l$  has a larger amplitude than  $\phi_h$ , which means the low energy particles are more sensitive to the solar activities. In the Zhu's model, if  $\phi_l$  is close to  $\phi_h$ ,  $R_b$  is too high or too low, the modified FFA model will be overfitting, and transform into FFA. There are also three parameters in Long's model:  $\phi_0$  and  $\phi_1$  to describe the linear relation between  $\phi(R)$  and  $\ln(R)$ , while g controls how much the drift processes affect the modulated spectrum. The model seems to be overfitting in 2014, 2016 and 2017, but it does not transform into FFA.

The Zhu's model and Long's model show very similar fitting results with mean  $\chi^2/d.o.f$  values of approximately 0.8, which are much better than the other two models. The two models prediction are very similar to each other, especially for the He/p ratio. The predictions both agree with the data within  $\pm$  5%, using the same parameters fitted with both protons and Helium simultaneously. Therefore, the data are consistent with the assumption that p and He undergo the same propagation processes in the heliosphere.

The results in this study verify that the modified FFA model is a valid parametrization of the GCR spectrum also at daily time scales. Usually, the FFA combined with GALPROP <sup>2</sup> (Strong & Moskalenko 1998; Moskalenko & Strong 1998) is used to constrain the origin and propagation of GCRs in the galaxy. In order to get better fitting results, different solar modulation parameters are adopted for different CR species (Yuan 2018). Actually, We need a

<sup>&</sup>lt;sup>2</sup> http://galprop.stanford.edu/

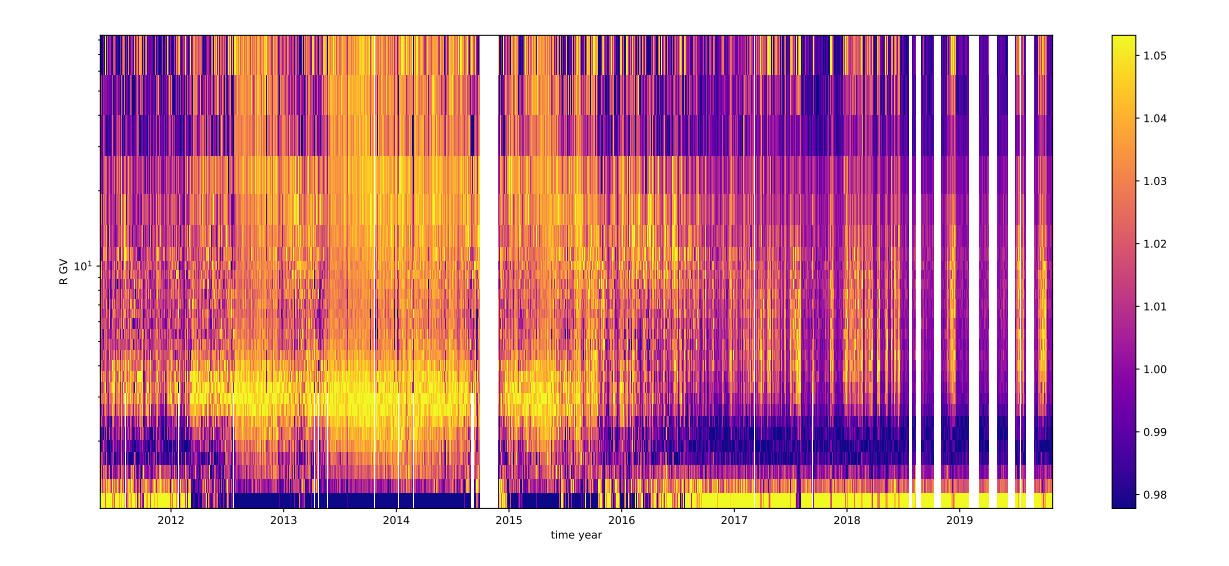


Figure 8. The ratio of Long's model prediction to data (model/data) for p fluxes of AMS-02 from may 2011 to may 2019

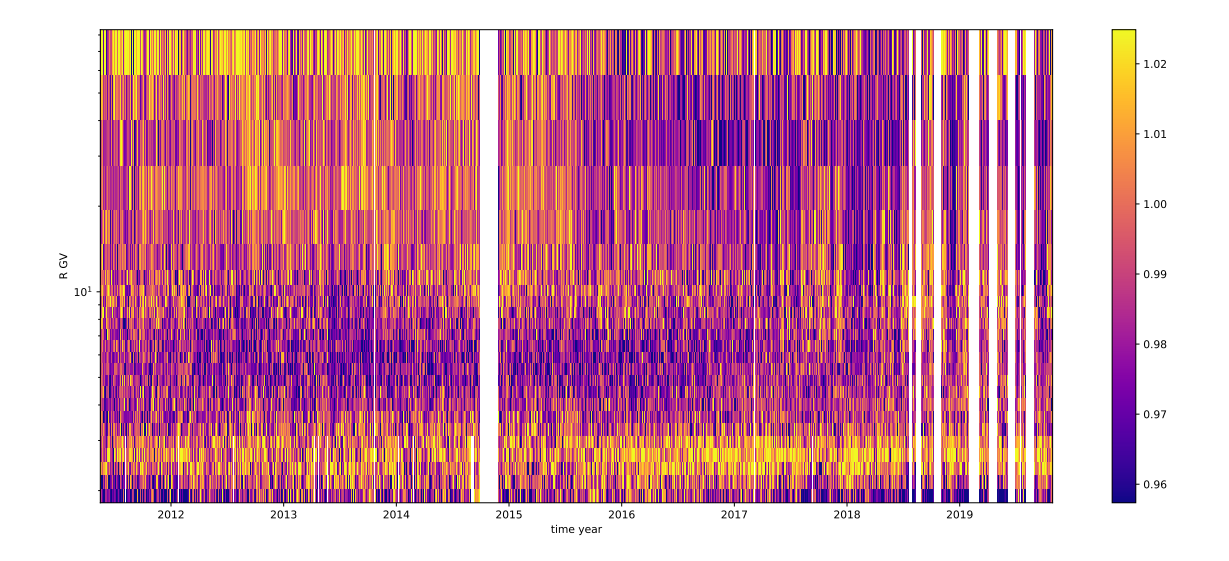


Figure 9. Same as 8 but for He.

sophisticated 3D time-dependent self-consistent model (Zhang 1999) to fully solve the problem related to cosmic ray transport in the heliosphere (Potgieter 2013). However it is too complex and computationally intensive to cooperate it with combination of GALPROP and MCMC (Yuan et al. 2017; Boschini et al. 2017). If we consider all the GCRs which have the same charge sign share the rigidity-dependent solar modulation potential in the study of propagation of GCRs in the galaxy, it will be useful to obtain the propagation parameters, as well as search for new physics such as dark matter signals in the antiproton flux. This can be tested by checking if the Zhu's and Long's models of modified FFA can reproduce daily AMS-02 positron data using the same modulation parameters as found by fitting p and He daily data. If so, the modulation parameters derived from daily AMS-02 electron data could be used to predict the time variation of anti-protons. This will be a subject of future studies.

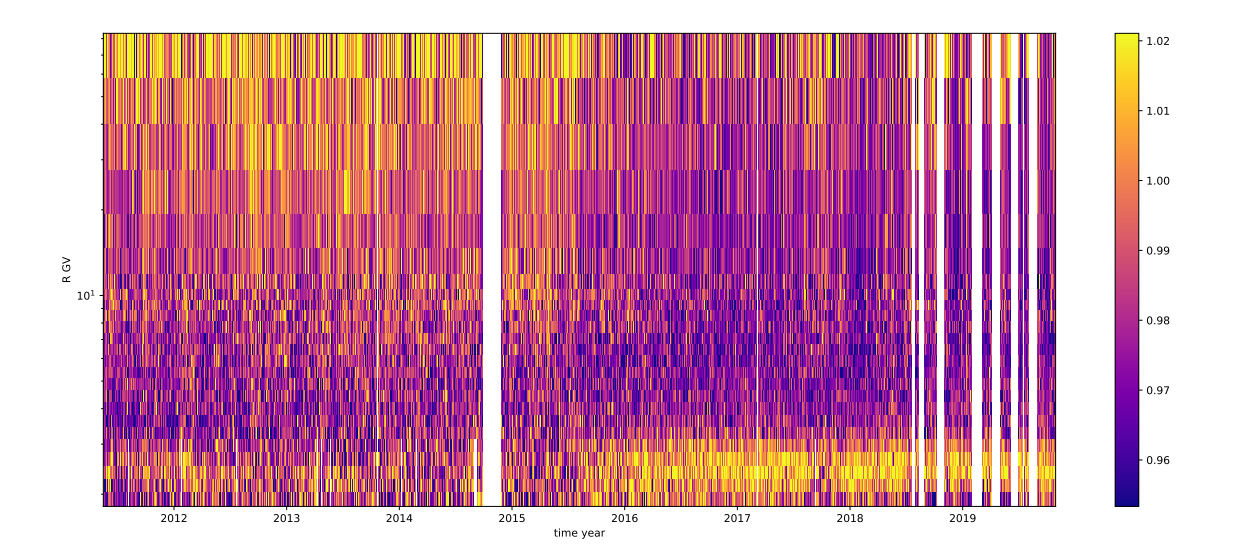


Figure 10. Same as 8 but for ratio of He/p.

- 1 Thanks for Qiang Yuan for very helpful discussions. This work is supported by the National Natural Science Foundation
- of China (No. 12203103). C.R.Z is also support by the Doctoral research start-up funding of Anhui Normal University.
- We acknowledge the use of the data from the Cosmic-Ray Database (https://tools.ssdc.asi.it/CosmicRays/) (Di Felice
- 4 et al. 2017).

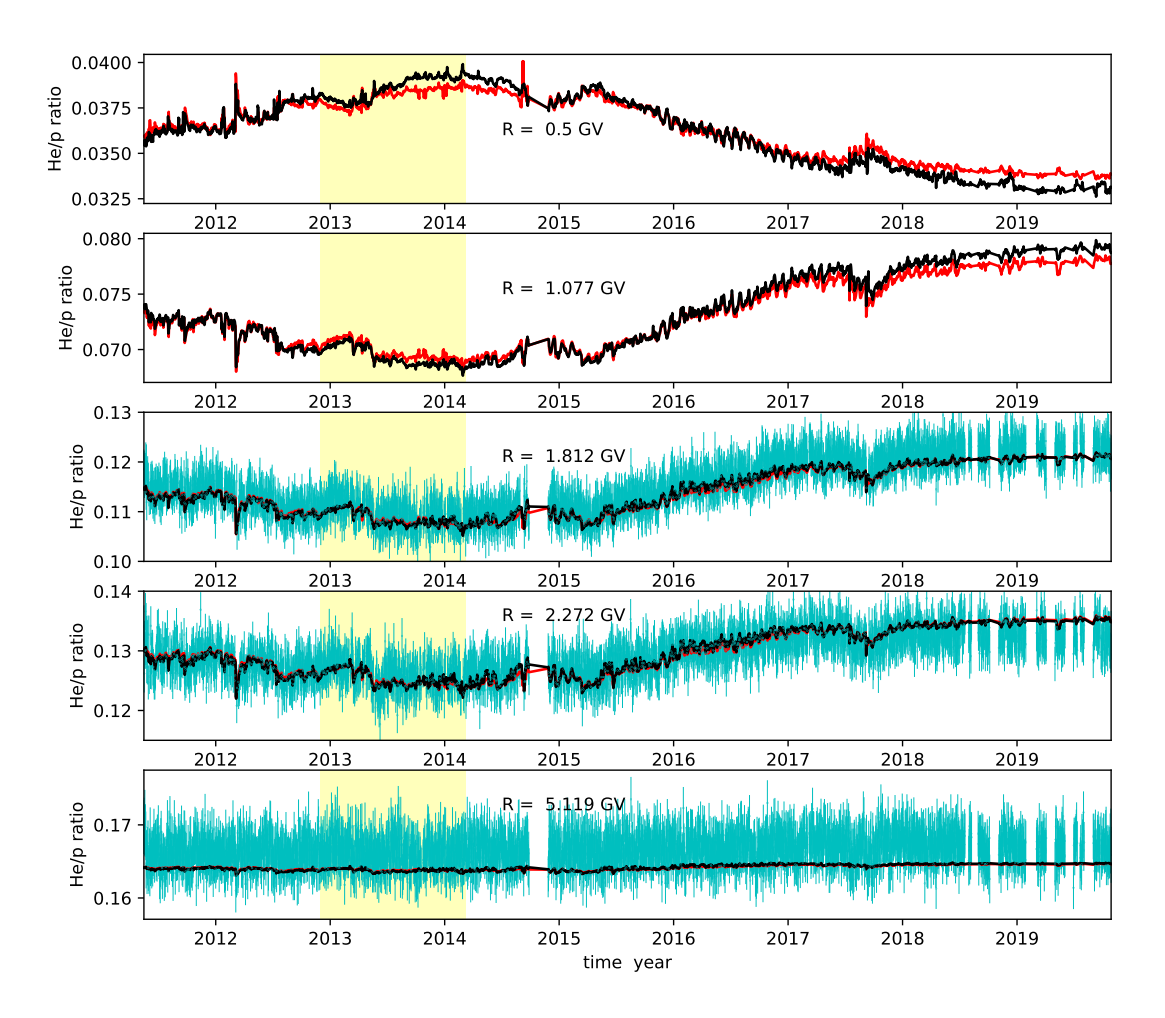


Figure 11. The best-fit time profiles of the Helium-to-proton ratio from Zhu's model (red) and Long's model (black) evaluated at rigidities R = 0.5 GV, 1.077 GV, 1.812 GV, 2.272 GV, and 5.119 GV (from top to bottom) are compared with the AMS-02 data (cyan).

### REFERENCES

- Adriani, O., Barbarino, G. C., Bazilevskaya, G. A., et al. 2011, Science, 332, 69, doi: 10.1126/science.1199172
- Aguilar, M., Ali Cavasonza, L., Alpat, B., et al. 2017, Phys. Rev. Lett., 119, 251101,
  - ${\bf doi:~10.1103/PhysRevLett.119.251101}$
- Aguilar, M., et al. 2021a, Phys. Rev. Lett., 127, 271102, doi: 10.1103/PhysRevLett.127.271102
- Aguilar, M., Ali Cavasonza, L., Ambrosi, G., et al. 2021b, Physics Reports, 894, 1,
  - doi: https://doi.org/10.1016/j.physrep.2020.09.003
- Aguilar, M., et al. 2022, Phys. Rev. Lett., 128, 231102, doi: 10.1103/PhysRevLett.128.231102
- Ambrosi, G., An, Q., Asfandiyarov, R., et al. 2017, Nature, 552, 63, doi: 10.1038/nature24475
- Bieber, J. W. 2003, Advances in Space Research, 32, 549, doi: 10.1016/S0273-1177(03)00338-7
- Blasi, P. 2013, Astron. Astrophys. ReV. , 21, 70, doi: 10.1007/s00159-013-0070-7
- Boschini, M., Della Torre, S., Gervasi, M., La Vacca, G., & Rancoita, P. 2018, Advances in Space Research, 62, 2859, doi: https://doi.org/10.1016/j.asr.2017.04.017
- Boschini, M. J., Della Torre, S., Gervasi, M., et al. 2017,Astrophys. J., 840, 115, doi: 10.3847/1538-4357/aa6e4f
- Caballero-Lopez, R. A., & Moraal, H. 2004, Journal of Geophysical Research: Space Physics, 109, doi: https://doi.org/10.1029/2003JA010098
- Cholis, I., Hooper, D., & Linden, T. 2016, Phys. Rev. D, 93, 043016, doi: 10.1103/PhysRevD.93.043016
- Cholis, I., Hooper, D., & Linden, T. 2022, Journal of Cosmology and Astroparticle Physics, 2022, 051, doi: 10.1088/1475-7516/2022/10/051
- Cholis, I., & McKinnon, I. 2022, Phys. Rev. D, 106, 063021, doi: 10.1103/PhysRevD.106.063021
- Corti, C., Bindi, V., Consolandi, C., & Whitman, K. 2016, Astrophys. J., 829, 8, doi: 10.3847/0004-637X/829/1/8
- Corti, C., Potgieter, M. S., Bindi, V., et al. 2019, The
   Astrophysical Journal, 871, 253,
   doi: 10.3847/1538-4357/aafac4
- Cui, M.-Y., Yuan, Q., Tsai, Y.-L. S., & Fan, Y.-Z. 2017, Phys. Rev. Lett., 118, 191101, doi: 10.1103/PhysRevLett.118.191101
- Cummings, A. C., Stone, E. C., Heikkila, B. C., et al. 2016, Astrophys. J., 831, 18, doi: 10.3847/0004-637X/831/1/18
- Di Felice, V., Pizzolotto, C., D'Urso, D., et al. 2017, PoS, ICRC2017, 1073, doi: 10.22323/1.301.1073
- Gamerman, D. 1997, Markov Chain Monte Carlo: Stochastic Simulation for Bayesian Inference (London: Chapman and Hall)

- Ghelfi, A., Barao, F., Derome, L., & Maurin, D. 2016, Astron. Astrophys., 591, A94, doi: 10.1051/0004-6361/201527852
- Ghelfi, A., Maurin, D., Cheminet, A., et al. 2017, Advances in Space Research, 60, 833–847, doi: 10.1016/j.asr.2016.06.027
- Gieseler, J., Heber, B., & Herbst, K. 2017, Journal of Geophysical Research (Space Physics), 122, 10, doi: 10.1002/2017JA024763
- Gleeson, L. J., & Axford, W. I. 1967, Astrophys. J. Lett., 149, L115, doi: 10.1086/180070
- —. 1968, Astrophys. J., 154, 1011, doi: 10.1086/149822
- Jokipii, J. R. 1971, Reviews of Geophysics and Space Physics, 9, 27, doi: 10.1029/RG009i001p00027
- Kuhlen, M., & Mertsch, P. 2019, Physical Review Letters, 123, doi: 10.1103/physrevlett.123.251104
- Lavalle, J., & Salati, P. 2012, Comptes Rendus Physique, 13, 740, doi: 10.1016/j.crhy.2012.05.001
- Lewis, A., & Bridle, S. 2002, Phys. Rev. D , 66, 103511, doi: 10.1103/PhysRevD.66.103511
- Li, J.-T., Beacom, J. F., & Peter, A. H. G. 2022, The Astrophysical Journal, 937, 27, doi: 10.3847/1538-4357/ac8cf3
- Liu, J., Yuan, Q., Bi, X.-J., Li, H., & Zhang, X. 2012, Physical Review D, 85, doi: 10.1103/physrevd.85.043507
- Long, W.-C., & Wu, J. 2024, Phys. Rev. D, 109, 083009, doi: 10.1103/PhysRevD.109.083009
- Luo, X., Potgieter, M. S., Bindi, V., Zhang, M., & Feng, X. 2019, The Astrophysical Journal, 878, 6, doi: 10.3847/1538-4357/ab1b2a
- Moskalenko, I. V., & Strong, A. W. 1998, The Astrophysical Journal, 493, 694–707, doi: 10.1086/305152
- Parker, E. N. 1965, Planet. Space Sci., 13, 9, doi: 10.1016/0032-0633(65)90131-5
- Potgieter, M. 2014, Brazilian Journal of Physics, 44, 581, doi: 10.1007/s13538-014-0238-2
- Potgieter, M. S. 2013, Living Reviews in Solar Physics, 10, 3, doi: 10.12942/lrsp-2013-3
- Shen, Z., Yang, H., Zuo, P., et al. 2021, Astrophys. J. , 921, 109, doi: 10.3847/1538-4357/ac1fe8
- Siruk, S., Kuznetsov, A., Mayorov, A., & Yulbarisov, R. 2024, Advances in Space Research, 74, 1978, doi: https://doi.org/10.1016/j.asr.2024.05.050
- Song, X., Luo, X., Potgieter, M. S., Liu, X., & Geng, Z. 2021, The Astrophysical Journal Supplement Series, 257, 48, doi: 10.3847/1538-4365/ac281c
- Strong, A. W., & Moskalenko, I. V. 1998, The Astrophysical Journal, 509, 212–228, doi: 10.1086/306470

- Strong, A. W., Moskalenko, I. V., & Ptuskin, V. S. 2007, Annual Review of Nuclear and Particle Science, 57, 285, doi: 10.1146/annurev.nucl.57.090506.123011
- Sun, X., Hoeksema, J. T., Liu, Y., & Zhao, J. 2015, Astrophys. J., 798, 114, doi: 10.1088/0004-637X/798/2/114
- Tomassetti, N. 2017, Phys. Rev. D, 96, 103005, doi: 10.1103/PhysRevD.96.103005
- Tomassetti, N., Barão, F., Bertucci, B., et al. 2018, Phys. Rev. Lett., 121, 251104, doi: 10.1103/PhysRevLett.121.251104
- Usoskin, I., Kovaltsov, G., Adriani, O., et al. 2015, Advances in Space Research, 55, 2940, doi: https://doi.org/10.1016/j.asr.2015.03.009
- Usoskin, I. G. 2017, Living Reviews in Solar Physics, 14, 3, doi: 10.1007/s41116-017-0006-9
- Usoskin, I. G., Gladysheva, O. G., Bobik, P., Kudela, K., & Kananen, H. 1999, Czechoslovak Journal of Physics, 49, 1743, doi: 10.1023/A:1022888121484

- Wang, B.-B., Bi, X.-J., Fang, K., Lin, S.-J., & Yin, P.-F. 2022, Phys. Rev. D , 106, 063006, doi: 10.1103/PhysRevD.106.063006
- Wang, S., Bindi, V., Consolandi, C., et al. 2023, The Astrophysical Journal, 950, 23, doi: 10.3847/1538-4357/acca1b
- Yuan, Q. 2018, Science China Physics, Mechanics and Astronomy, 62, doi: 10.1007/s11433-018-9300-0
- Yuan, Q., & Bi, X.-J. 2015, JCAP, 03, 033, doi: 10.1088/1475-7516/2015/03/033
- Yuan, Q., Lin, S.-J., Fang, K., & Bi, X.-J. 2017, Phys. Rev. D , 95, 083007, doi: 10.1103/PhysRevD.95.083007
- Zhang, M. 1999, Astrophys. J., 513, 409, doi: 10.1086/306857
- Zhu, C.-R. 2024, The Astrophysical Journal, 975, 270, doi: 10.3847/1538-4357/ad794b
- Zhu, C.-R., Cui, M.-Y., Xia, Z.-Q., et al. 2022, Phys. Rev.
  Lett., 129, 231101, doi: 10.1103/PhysRevLett.129.231101
  Zhu, C.-R., Yuan, Q., & Wei, D.-M. 2021, Astropart. Phys.,

 $124,\,102495,\,\mathrm{doi}\colon 10.1016/\mathrm{j.astropartphys.}2020.102495$